

# Effects of Force Distribution and Rebound on Electromagnetically Formed Sheet Metal

J. Imbert<sup>1</sup> , M. Worswick<sup>1</sup> and P. L'eplattenier<sup>2</sup>

<sup>1</sup> Department of Mechanical and Mechatronics Engineering, University of Waterloo, 200 University Avenue West, Waterloo, Ontario, Canada, N2L-3G1

<sup>2</sup> Livermore Software Technology Corporation, 7374 Las Positas Road, Livermore, CA 94550

## Abstract

*Electromagnetic forming (EMF) is a high speed forming process that has been shown to increase the formability of aluminum alloys under certain conditions. Many authors have reported significant increases in formability; however, there is as of yet no complete understanding of the process. Obtaining a gain in formability is not the only factor that must be considered when studying EMF. The process rapidly generates significant forces which lead to the deformation of the material at very high rates. The applied forces depend on the shape of the electromagnetic coil used, which leads to force distributions that may not be ideal for forming a particular part. Once the sheet is accelerated it will travel at high speeds until it impacts the die. This high speed impact results in the sheet rebounding from the die. Both the force distribution and the rebound affect the final shape of the part. This paper presents the results of experimental and numerical study carried out to determine the effect of the force distribution and the rebound on samples of conical and "v-channel" geometry. It was found that both sample geometries are affected by the force distribution and the rebound, with the v-channel samples being considerably more affected. The results indicate that these effects must be carefully considered when EMF processes are designed..*

## Keywords

Metal, Forming, Electro-magnetic, High, Speed.

## 1 Introduction

Interest in electromagnetic forming (EMF) of sheet metal for automotive applications has been growing in recent years, due to its potential as a means of forming aluminum and other low formability materials. Forming of aluminum has been the main focus, due to its inferior forming characteristics relative to mild steel [1,2,3] and its relatively high conductivity.

Despite having been in use since the early 1960's [4], there is not yet a complete understanding of EMF. Progress has been made since the mid-1990's in this regard [5-13]; however, there is still not sufficient knowledge of this process to be able to properly design EMF processes for industrial sheet metal forming applications.

Obtaining the desired shape of a part within the specified tolerances is the goal of any forming operation. In conventional forming, the punch and die produce the final shape, with springback being the principal factor that may cause deviations from the desired final shape. Designers must account for spring back by modifying the design of the tools to achieve the desired part geometry. EMF differs significantly in that the punch is replaced by the forces induced on the sheet by the coil, which propel the sheet at high speeds into a die shaped in such a way as to provide the final part. Ideally, after the process is complete the material emerges with the final shape. Unfortunately, in EMF the force distribution generated on the sheet by the coil and the rebound caused by the impact of the sheet with the die can produce parts that deviate from the specified shapes. Imbert et al. [11] reported that samples formed with aluminum alloy sheets into a conical die, did not conform to the die shape. A step was generated on the part, which was attributed to the rebound of the sheet. Risch et al. [14-16] studied the effects of the rebound on axisymmetric parts and suggested design changes in the part and die to alleviate the deformation caused by the rebound.

This paper presents the results of a study conducted on the effects of force distribution and rebound on the final shape of samples formed using EMF. Conical and open channel samples were formed from 1 mm sheet of AA 5754, which is an aluminum alloy in relatively widespread use in the automotive industry. These shapes were chosen since the cone has substantially greater geometric stiffness than the open channel geometry, which means that the conical shapes will be harder to deform. By using this approach, two extreme cases could be studied that would provide information on typical forming operations, since the response of typical manufactured parts will likely fall between those of these two geometries. The samples were formed using two different coils; the conical samples were formed with a spiral coil, while the open channel v-cross section samples were formed with a rectangular coil. The final shapes of the samples are presented to show the effects of the pressure distribution and the rebound. Numerical analysis was carried out to compliment and better understand the experiments. The analysis was carried out with a commercially available coupled code capable of simultaneously solving the electromagnetic and structural problem.

## **2 Experimental Procedure**

### **2.1 Conical Samples**

The conical samples were formed as part of the work described in [17], which provides details of the experimental procedures. Cones were formed with side angles of 34, 40 and 45°. The conical samples were formed using a 7-turn spiral coil with a nominal diameter of 100 mm and a maximum diameter of 115 mm. An IAP Magnepress [18] magnetic pulse generator with a storage capacity of 22.5 kJ at 15kV was used to form the samples. The material was clamped to the die and a vacuum drawn to remove the trapped air.

## 2.2 Open Channel Samples

The open channel samples were formed into a “V” shaped die (Figure 1). The side angle of 40° was chosen since it was the maximum angle reached with no failure for the conical samples [17]. The open channel samples were formed using a double pancake coil made from 4.6 mm (0.180 in) square copper rod, with each side of the coil having six turns (Figure 2). The coil was connected to a Pulsar [19] MPW 20 – Research Edition magnetic pulse generator, which consists of a capacitor bank and a power supply to deliver the current to the capacitors at the required specifications. The power supply has a nominal maximum energy capacity of 20 kJ and charging voltage of 9 kV. The samples for this work were formed using 3 and 5 kV, which gave storage energies of 2.48 and 6.73 kJ respectively.

**Figure 1:** Drawing of the stool used to form the v-channel samples, together with a schematic showing the coil position and a highly simplified pressure distribution over the area of the sample that deforms during the process.

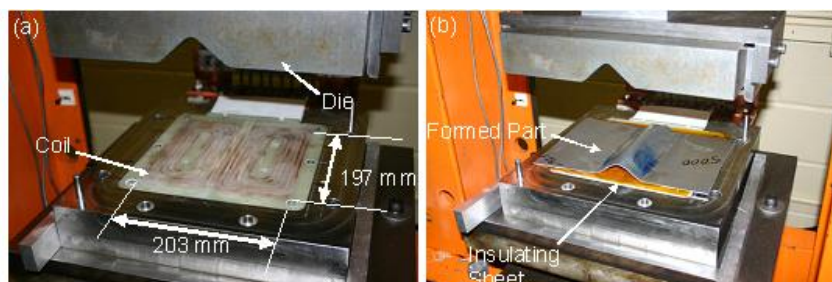


**Figure 2:** Tooling used for the experiment a) coil and die and b) tooling with a formed part and insulating sheet.

The material tested was 1 mm AA 5754 in samples of 197 x 305 mm. The material was formed by placing over a coil that was connected to the pulse generator. The coil was encased in epoxy to provide insulation and structural strength. Additional insulation was provided by sheets of an insulating material (Kapton™). The insulating materials resulted in a separation between the sheet and the coil of approximately 1 mm. The sheet and die were held in place by the force provided by the hydraulic press.

## 3 Numerical Analysis

It is very difficult to measure experimentally the deformation history, the currents and the Lorentz forces induced on the sheet in EMF, due to the high speed nature of the process and the closed tools that are used. The experiments were modelled numerically to gain some insight on the parameters mentioned above. The numerical effort for this work was undertaken with a version of LS-DYNA which can model the EM and structural parts of the problem. The software performs the EM calculations by using both Finite Element Analysis (FEA) and the Boundary Element Method (BEM) to solve Maxwell's equations in

the eddy-current approximation. FEA is used to solve the EM equation in the conductors (e.g. coil and workpiece) and the BEM is used to model the air. By using the BEM to model the air, the small and distorted elements that can result when small air gaps exist between the coil and workpiece are eliminated. The major drawback of this approach is that it is very memory and processor-time intensive. A detailed description of the method is provided in [20]. A study performed to validate the software is presented in [21].

The coil and workpiece were modelled using eight node hexahedral solid elements. Solid elements are required for both electromagnetic and structural calculations, to solve the induced currents and to capture the through thickness and shear stresses on the sheet during forming [11]. The sheet was modeled with an elastic-plastic piece-wise-linear plasticity model that is incorporated into LS-DYNA [22] with a quasi-static stress-strain flow curve (Figure 3). The details of this particular implementation are described in [17]. The coils were modeled as elastic materials. Tooling components were modelled as rigid bodies and their surfaces were discretised using shell elements for the structural calculation. The tool elements were ignored for the electromagnetic calculation. The mesh for the conical samples is shown on Figure 4 and for the v-channel on Figure 5.

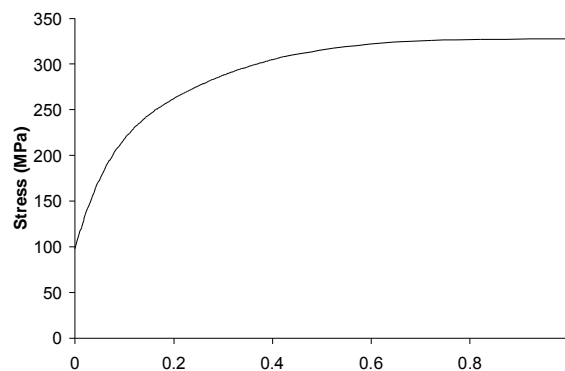


**Figure 3:** Quasi-static true stress-strain data for AA5754 used in the numerical model.

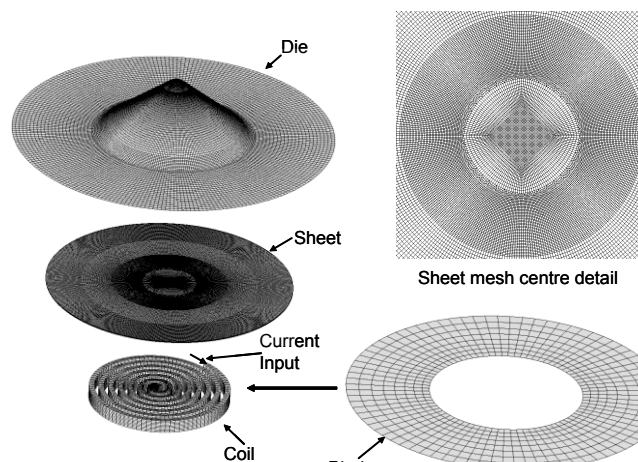


**Figure 4:** Mesh for the conical sample models. The binder lies between the coil and the sheet and, together with the die, clamps the sheet. Neither the die and binder meshes are included in the EM calculations.

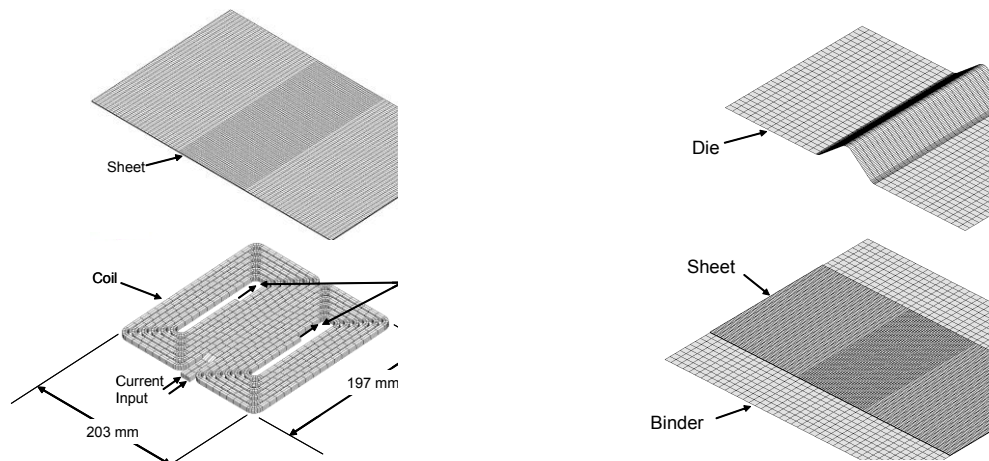


**Figure 5:** Meshes for the V-channel models. The binder and the die are used to clamp the sheet in place.

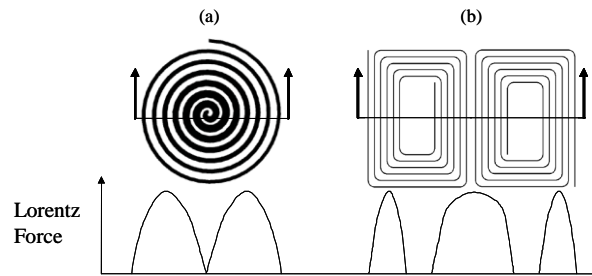
For the conical simulations, the sheet meshes were composed of 258,560 elements, while the sheet mesh for the v-channel simulations had 28,800 elements. The much larger number of elements for the cone mesh was needed to accurately capture the features found in the experimental results and to avoid erroneous predictions due to element geometry [17]. Utilizing more elements might have resulted in more accurate results; however, the memory limits of the computers being used was exceeded when more elements were used.

To reduce run times the EM part of the solver was not active for the whole simulation, it was deactivated after the induced forces became negligible. For the V-Channel models the run total time was 400  $\mu\text{s}$ , with the EM module turned off after 50  $\mu\text{s}$ . For the conical model the total run times were 200  $\mu\text{s}$  and the EM module was deactivated at 25  $\mu\text{s}$ .

The simulations captured the general behaviour of both forming operations. The observed discrepancies described below are believed to be caused by the material model, the coarseness of the sheet mesh (especially for the v-channel samples) and the imperfections of the coil that were not reproduced in the model.

## 4 Effect of Force Distribution

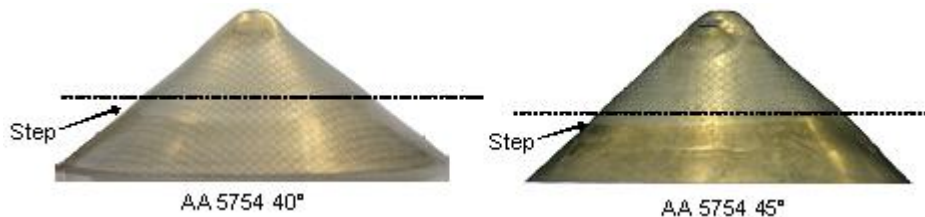
In EMF, the force on the sample is the result of the repelling magnetic fields of the coil and those of the induced eddy currents in the sheet. Since the path of the eddy currents will be opposite to the path of the current flowing through the coil, the eddy currents and the force distribution on the sample will be dictated by the shape of the coil. Practical limitations such as the provision of an adequate current path, ease of manufacture, structural strength and magnetic properties of the coil result in shapes that may not produce the ideal force distributions. Also, the sharp edges of the blank can produce current concentrations that will increase the induced force at the edges of the sample and consequently result in larger local deformations. The net result is a force distribution that may not be ideal for a particular forming process. The specimens studied in this work were formed using spiral (conical sample) and rectangular “double pancake” (v-channel) coils, which are illustrated schematically with approximate force distributions on Figure 6.



**Figure 6:** Schematic of a) spiral and b) rectangular “double pancake” coil with approximate force distributions along the centreline.

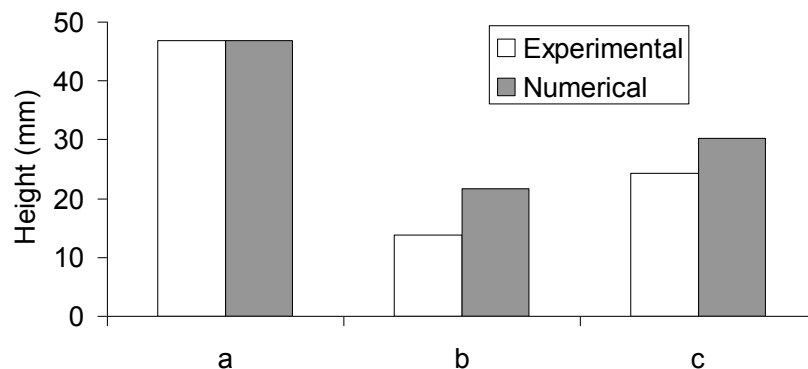
#### 4.1 Conical Samples

Figure 7 shows representative as-formed conical samples. The heights for the samples were 46.9 mm and 54.4 mm, for the 40° and 45° cones respectively. It can be seen that the parts do not form a perfect cone. A prominent feature present is the step that can be seen on both samples, in addition to distortion at the top of the cone. The step is attributed to the rebound and will be discussed below. The step can be used to visualize the uneven forming that is the result of the pressure distribution. It can be seen that the step for the 45° sample is not horizontal, which is a result of the force distribution. The 40° sample shown also has a non-horizontal step, but it is less prominent than the step of the 45° sample.



**Figure 7:** Conical samples showing the step formed due to the rebound. Note that the step for the 45° samples is more inclined.

The 40° conical sample experiments were modelled and the software was able to capture the expected behaviour for a sample formed using a spiral coil. The sample heights were very accurately predicted which was expected since the samples filled the die and did not vary drastically from the final shape. Figure 8 shows a comparison between the experimental and predicted heights for the conical and v-channel samples.



**Figure 8:** Experimental and numerical sample heights for a) the 40° conical samples, b) v-channel samples with no die contact and c) v-channel samples with die contact.

Figure 9 shows the predicted force distribution produced on a sheet; which is characterized by a zone of zero induced force near the centre. Spiral coils are usually assumed to be axi-symmetric in many analyses. Using this assumption they produce axi-symmetric current and force distributions, which is a simplification of the actual distributions. The result of the non-uniform force distribution is that the material fills the die unevenly producing a non-uniform strain distribution and surface features, as shown on Figure 10. The results for the 45° samples were not included due to the fact that failure was observed in the experiments and the numerical model was not able to capture the failure modes.

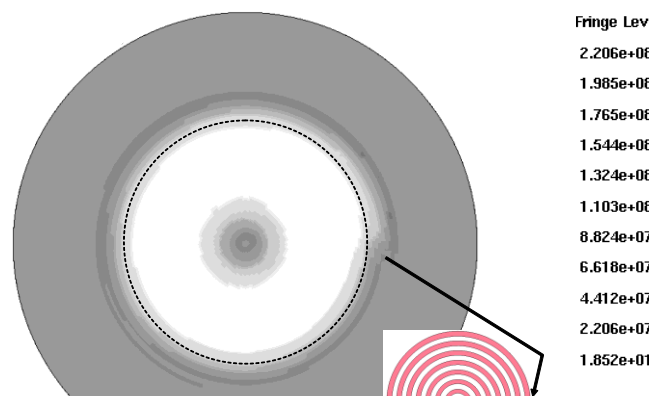


**Figure 9:** Predicted current density produced by a spiral coil on a flat sheet. The broken-line circle is placed to highlight the non-uniformity of the field. Fringe levels are of Lorentz force in  $\mu\text{N}$ .

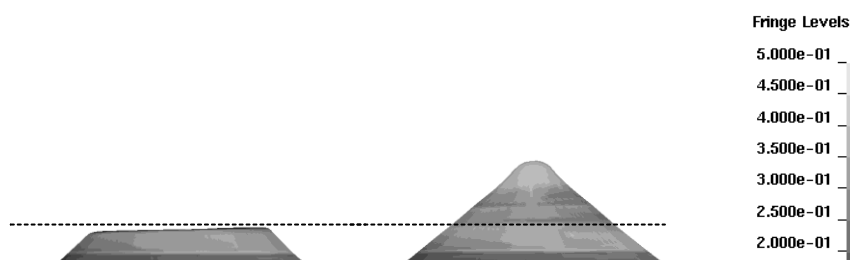


**Figure 10:** Conical die modelling results. The contours are of effective plastic strain.

## 4.2 V-Channel Samples

Samples that did not make contact with the dies were formed using the v-channel apparatus to isolate the effects of the force distribution from the effects of the impact of the sheet with the die. A representative sample formed is shown on Figure 11. It can be clearly seen that the part does not have a uniform height. The final shape is the result of the non-uniform force distribution produced by the coil. It can be seen that the height varies along the length of the part, with the centre of the part being the highest point. The average height for three experimental samples is 13.8 mm. This height distribution is

consistent with the predicted force distribution shown on Figure 12. The right side of the sample is higher than the left, due to higher forces acting on that side of the sheet, which are the result of irregularities in the coil. These irregularities result in the coil being slightly more separated from the sheet on the side with the lower height. Towards the ends of the part there is a reduction in height which is consistent with the geometry of the coil and the predicted force distribution which will be discussed below. At the ends of the samples the height stops decreasing and increases at the very edge, this is likely due to the concentration of the current produced at the edges, which results in a local increase in Lorentz forces.

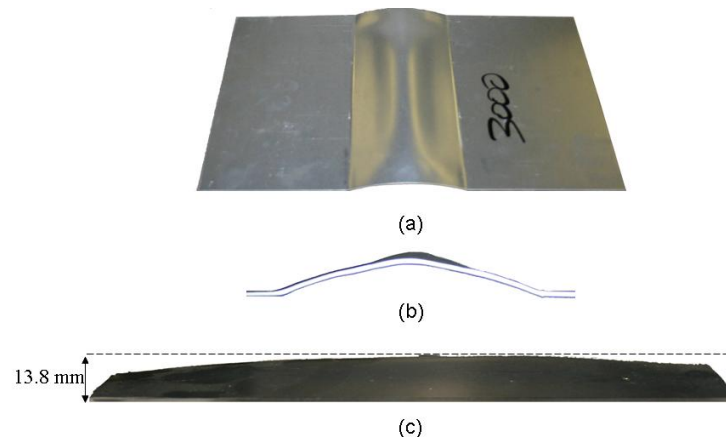


**Figure 11:** Part formed using a charging voltage of 3000 volts and the double pancake coil, a) view from above and b) front view.

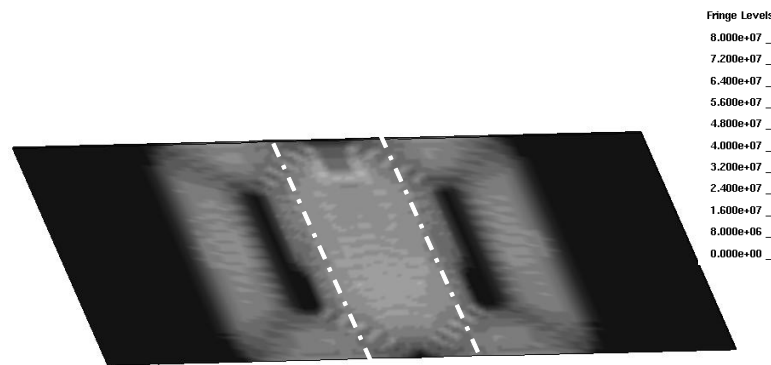


**Figure 12:** Predicted force distribution on the sheet. Fringe levels are of Lorentz force in  $\mu\text{N}$ . The broken white lines indicate the approximate location of the die cavity.

The predicted final shape for this experiment is shown on Figure 13. The maximum predicted height is 21.6 mm which is 38% higher than the actual height of the samples (Figure 8). This over prediction is likely due to the material model used and to the fact that the numerical coil has an ideal shape that does not take into account the imperfections of the actual coil. Thus, the coil is uniformly separated from the sheet, which results in higher induced forces when compared to the experiments. Another consequence of the numerical coils ideal shape is that the predicted shape is symmetric and does not exhibit the significant difference in height from one end to the other of the sample present in the actual samples. The models predict the raised edges which are observed in the actual samples. The predicted strain distributions are non uniform, which is an expected result given the force distribution.



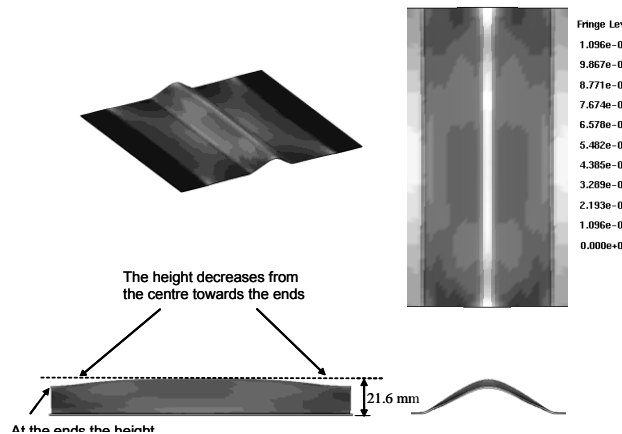


**Figure 13:** Final predicted v-channel shape for a sample that makes no contact with the die (3000 V charging voltage). The general trends in the height are predicted by the model.

## 5 Rebound of the Sheet

When the sheet impacts the die, not all of the kinetic energy results in plastic deformation, thus some of the energy is expended by causing the sheet to rebound off the die wall. The principal effect of this rebound is that the parts do not conform to the die shape. Both the conical and v-channel samples show clear evidence of this rebound, with greater rebound being observed in the latter due to its lower stiffness.

### 5.1 Conical Samples

The rebound in the conical samples causes a distinctive “step” which can be seen on Figure 7. Numerical models of conical samples formed using an axisymmetric pressure distribution predict the formation of a step, thus it is believed that the step is caused by the rebound. Although the step may not be a significant issue for some structural applications, it could be aesthetically displeasing and render a part unfit if the appearance is an important criterion, such as a “class A” automotive surface. The steps present in the experimental samples were not usually horizontal. This was due to the uneven pressure distribution discussed above. Due to the more constrained nature of the conical parts and the more uniform pressure distribution provided by the spiral coil used in that work, the discrepancy between the final part and die were not as great as those that have been observed with the v-channel samples, which will be discussed next.

### 5.2 V-Channel Samples

A representative sample formed with the single cavity die is shown on Figure 14. Blue ink was applied to the surface of the die to confirm that the sheet impacted the die during the experiment. After forming, the samples showed clear indications of impact. The dark areas that can be seen on the part shown on Figure 14 are stains left by the ink from the die that indicate where the sheet contacted the tool. The rebound in the v-channel samples was significantly more pronounced than in the conical samples. It is clear that after impact the sheet rebounded from the die surface to form the final shape. In contrast

to the conical samples, the parts formed with the v-channel differ significantly from the shape of the die. The highest point on the samples was offset to the right of the die, as is shown on Figure 14. The average maximum final height of the samples was 24.3 mm.

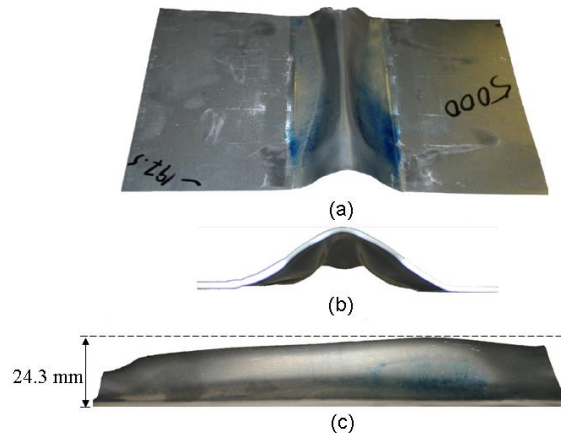


**Figure 14:** Part formed using a charging voltage of 5000 volts, a) view from above, b) front view c) side view. The blue markings in a) indicate where the sheet made contact with the die.

The rebound is predicted by the numerical analysis, although with less severity than is actually observed (Figure 15). This effect of the EM field is negligible for the impact event, since by the time the sheet impacts the die the EM forces are not significant. In fact, in the numerical simulations the EM solver is not active when the rebound occurs. The severity of the rebound will depend on the velocity, and thus the EM force that was induced on the sheet. Therefore, non-uniform force distributions will result in uneven rebound, which can be seen in the part shown on Figure 13. The model did not predict the exact height distribution seen on the samples nor the final maximum height (Figure 8). The final shape of the predicted samples showed an apparent reversal in the height distribution, with the highest points occurring towards the ends. This results from the sheet rebounding after impact. Figure 13 shows the sample geometry just before impact, and it can be seen that the height distribution is essentially the same as for the no-impact sample. The centre of the part is not only the highest point, but also the fastest moving. Therefore, when it impacts the die the rebound is greater than the ends of the part, and this effect was exaggerated in the numerical model. Finally, the effects of the edges are less evident in the model results, but are still present.

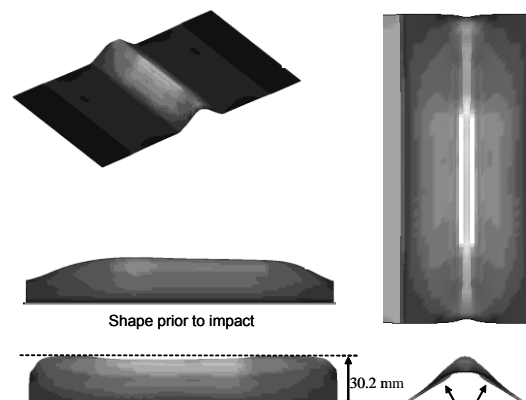


**Figure 15:** Final predicted v-channel shape for sample with rebound present (5000 V charging voltage).

## 6 Conclusions

Magnetic force distribution and rebound have a significant impact on the final shape of electromagnetically formed parts and must be considered when designing EM forming processes. One approach to eliminate the force distribution effects would be to use a coil that produces a uniform pressure distribution, like the one proposed by Kamal and Daehn [23]. If coils with non-uniform force distributions have to be used, the force distributions can be predicted from the shape of the coil using analytical approximations or they can be much more accurately determined from numerical analysis. Knowledge of this distribution can, in principle, be used to adjust the die and blank to obtain the desired final shape.

The rebound of the sheet can be a potentially more difficult challenge. Numerical models can be used to determine the general final shape of the part. However, to obtain an accurate solution reliable code and accurate material models are needed. The greatest challenge will be designing the coil, blank and die to try and minimize rebound. Some suggestions have been made in the literature, such as energy absorbing dies [14]; however, these solutions have significant practical challenges. Possibly the most significant amongst these challenges is how to make the dies economically feasible.

Both the force distribution and rebound can lead to final part shapes and surface conditions that could lead to parts that do not meet specifications. Understanding these effects is very important for the practical implantation of EMF. Further study is required to fully understand these effects.

## References

- [1] *Wilson, D.V.*, 1988. Aluminium versus steel in the family car-The formability factor”, *Journal of Mechanical Work Technology*, 16, 1988, 257-277.
- [2] *Miller W.S.; Zhuang L.; Bottema J.; Wittebrood A.J.; De Smet P.; Haszler A.; Vieregge A.*, 2000. Recent development in aluminium alloys for the automotive industry. *Material Science Engineering A280*, 37-49.
- [3] *Mori, T., Hino, M., Iwaya, J., Miyahara, M.*, 1992. Press formability of aluminum alloy sheets for automobile parts”, *KOBELCO Technology Review*, 14, 49-53.
- [4] *Wagner, H.J., Boulger, F.W.*, 1960. High velocity metalworking processes based on the sudden release of electrical of electrical energy. Memorandum prepared by the Battle Memorial Institute for the Defense Metals Information Center.
- [5] *Altynova, M., Hu, X., Daehn, G.S.*, 1996. Increased ductility in high velocity electromagnetic ring expansion, *Metallurgical and Material Transactions A*, 27A, 1837-1844.
- [6] *Balanethiram, V.S., Daehn, G.S.*, 1994. Hyperplasticity: Increased forming limits at high workpiece velocity. *Scripta Metallurgica et Materialia*, 30, 515-520.
- [7] *Daehn, G.S., Vohnout, V.J., DuBois, L.*, Improved Formability with Electromagnetic Forming: Fundamentals and Practical Example. Proceedings of the TMS Sheet Metal Forming Symposium, San Diego, Ca., TMS, February 1999.
- [8] *Oliveira, D.A., Worswick, M.J.*, 2003. Electromagnetic forming of aluminum alloy sheet”, *Journal de Physique IV*, 110, 293-298.

- [9] *Golovashchenko, S.F., Mamutov, V.S., Dmitriev, V.V., Sherman, A.M., 2003.* Formability of sheet metal with pulsed electromagnetic and electrohydraulic technologies. In: Das, S.K. Proceedings of the TMS annual meeting, San Diego, Ca., TMS, pp. 99-110.
- [10] *Golovashchenko, S.F., 2007.* Material Formability and Coil Design in Electromagnetic Forming. *Journal of Materials Engineering and Performance*, 16, 314-320.
- [11] *Imbert, J.M., Worswick, M.J., Winkler, S.L., Golovashchenko, S., Dmitriev, V., 2005.* Analysis of the Increased Formability of Aluminum Alloy Sheet Formed Using Electromagnetic Forming . SAE Transactions, International Journal of Materials and Manufacturing. SAE paper number 2005-01-0082
- [12] *Imbert, J.M.; Winkler, S.L; Worswick, M.; Oliveira, D.A. and Golovashchenko, S., 2005.* The Effect of Tool/Sheet Interaction on Damage Evolution in Electromagnetic Forming of Aluminum Alloy Sheet. *Journal of Engineering Materials Technology* 127/1, 145-152.
- [13] *Seth, M., Vohnout, V.J., Daehn, G., 2005.* Formability of steel sheet in high velocity impact. *Journal of Materials Process Technology*, 168/3, p 390-400.
- [14] *Risch, D., Beerwald, C., Brosius, A., Kleiner, M., 2004.* On the Significance of the Die Design for Electromagnetic Sheet Metal Forming. In: Kleiner, M., Proceedings of the 1<sup>st</sup> International Conference on High Speed Forming, Dortmund, Germany, pp. 191-200.
- [15] *Risch, D., Vogil, E., Bauman, I, Brosius, A., Beerwald, C., Tillman, W. Kleiner, M., 2006.* Aspects of Die Design for the Electromagnetic Sheet Metal Forming Process. In: Kleiner, M., Proceedings of the 2nd International Conference on High Speed Forming, Dortmund, Germany, pp. 189-199.
- [16] *Risch, D., Brosius, A., Kleiner, M., 2007.* Influence of the Workpiece Stiffness on the Electromagnetic Sheet Metal Foming Process into Dies. *Journal of Materials Engineering and Performance*, 16, 327-330.
- [17] *Imbert, J., 2005.* Increased Formability and the Effects of the Tool/Sheet Interaction in Electromagnetic Forming of Aluminum Alloy Sheet. University of Waterloo M.A.Sc. thesis. <http://etd.uwaterloo.ca/etd/jmsimber2005.pdf>.
- [18] IAP Research, 2006. Dayton, OH, USA, [www.iap.com](http://www.iap.com).
- [19] Pulsar, 2006. Yavne, Israel. [www.pulsar.co.il](http://www.pulsar.co.il).
- [20] *L'Eplattenier, P., Cook, G., Ashcraft, C., Burger, M., Shapiro, A., Daehn, G., Seth, M., 2006.* Introduction of an Electromagnetism Module in LS-DYNA for Coupled Mechanical-Thermal-Electromagnetic Simulations. In: 9<sup>th</sup> International LS-DYNA Users Conference.
- [21] *Imbert, J.M.; L'Eplattenier, P., and Worswick, M., 2008.* Comparison Between Experimental and Numerical Results of Electromagnetic Forming Processes. In: Mindle, W., Proceedings of the 10<sup>th</sup> International LS-DYNA Users Conference 2008, Dearborn, Michigan, pp. 12-33-12-44.
- [22] *Hallquist, J., 1998.* *LS-DYNA Theoretical Manual*, Livermore software Technology Corporation.
- [23] *Kamal, M. and Daehn, G. S. , A uniform pressure electromagnetic actuator for forming flat sheets, Journal of Manufacturing Science and Engineering, Transactions of the ASME, v 129, n 2, p 369-379, 2007.*